Energy Dependence of the NN t-matrix in the Optical Potential for Elastic Nucleon-Nucleus Scattering

Ch. Elster, S.P. Weppner

Institute of Nuclear and Particle Physics, and Department of Physics,
Ohio University, Athens, OH 45701

(February 9, 2008)

Abstract

The influence of the energy dependence of the free NN t-matrix on the optical potential of nucleon-nucleus elastic scattering is investigated within the context of a full-folding model based on the impulse approximation. The treatment of the pole structure of the NN t-matrix, which has to be taken into account when integrating to negative energies is described in detail. We calculate proton-nucleus elastic scattering observables for ^{16}O, ^{40}Ca, and ^{208}Pb between 65 and 200 MeV laboratory energy and study the effect of the energy dependence of the NN t-matrix. We compare this result with experiment and with calculations where the center-of-mass energy of the NN t-matrix is fixed at half the projectile energy. It is found that around 200 MeV the fixed energy approximation is a very good representation of the full calculation, however deviations occur when going to lower energies (65 MeV).

Typeset using REVTEX

I. INTRODUCTION

The scattering of protons and neutrons from nuclei has a long history as a tool to investigate the details of the reaction mechanism between a nucleon and a many nucleon system. The spectator expansion of multiple scattering theory [1–3] is our theoretical approach to define an optical potential for elastic nucleon-nucleus scattering. This expansion is predicated upon the idea that two-body interactions between projectile and target nucleons play the dominant role.

In its most general form, the first order single scattering optical potential within the framework of the spectator expansion is given by the expectation value of the nucleon-nucleon (NN) transition amplitude and the ground state of the target nucleus. This 'full-folding' optical potential involves the convolution of the fully-off-shell two nucleon scattering amplitude with a realistic nuclear density matrix. In this form, the exact calculation of this optical potential requires a three-dimensional integration, in which the integration variable is coupled to the energy of propagation of the projectile and target nucleon. This very fact leads to a full-folding optical potential, which explicitly treats the off-shell behavior *and* the energy dependence of the NN t-matrix when carrying out the integration. Full-folding models along this line have been proposed and carried out [4,5] with the conclusion that these model calculations based on the free NN t-matrix give a good description of the data for energies between 200 and 400 MeV, however are rather poor at 200 MeV and below. We have repeated these calculations within our computational framework based on a full-folding model employing a realistic nuclear density matrix and a free NN t-matrix where the off-shell behavior as well as the energy dependence are taken into account. However, we do not find as large effects as shown in Refs. [4,5].

It can be argued that at intermediate energies the scattering of a projectile from a nucleon in the target nucleus may resemble free NN scattering mainly in forward direction. This is the justification for a common approximation to the optical potential in which the energy of the NN t-matrix is uncoupled from the integration variable by fixing it at half the projectile laboratory energy. We will study the accuracy of this assumption at different projectile energies.

The structure of this paper is as follows. First we will review in Section II the relevant expressions for the single scattering optical potential in the impulse approximation as well as the full-folding procedure as used in our calculations. We will describe in some detail the numerical implementation for treating the energy dependence of the NN t-matrix, especially since this was left out in Ref. [4]. We then present in Section III elastic scattering results for proton scattering from a variety of nuclei in the energy regime between 65 and 200 MeV, and end with concluding remarks in Section IV.

II. THEORETICAL FORMULATION

The transition amplitude for elastic scattering of a projectile from a target nucleus is given as [3]

$$T_{el} = PUP + PUG_0(E)T_{el}, \tag{2.1}$$

where P is the projector on the ground state $|\Phi_A\rangle$ of the target, $P = \frac{|\Phi_A\rangle\langle\Phi_A|}{\langle\Phi_A|\Phi_A\rangle}$, and $G_0(E) = (E - H_0 + i\varepsilon)^{-1}$. For the scattering of a single particle projectile from an A-particle target nucleus the free Hamiltonian is given by $H_0 = h_0 + H_A$, where H_A stands for the target Hamiltonian. In the spirit of the spectator expansion the target Hamiltonian is viewed as $H_A = h_i + \sum_{j\neq i} v_{ij} + H^i$, where h_i is the kinetic energy operator for the ith target nucleon, v_{ij} the interaction between target nucleon i and the other target nucleons j, and H^i is an (A-1)-body operator containing all higher order effects. In a mean field approximation $\sum_{j\neq i} v_{ij} \approx W_i$, where W_i is assumed to depend only on the ith particle coordinate. Thus, the propagator consistent with the first order in the spectator expansions is given as

$$G_0(E) \approx G_i(E) = [(E - E^i) - h_0 - h_i - W_i + i\varepsilon]^{-1}. \tag{2.2}$$

Here H^i, having no explicit dependence on the ith particle, is replaced by an average energy E^i, which is at most equivalent to the separation energy of a nucleon from the nucleus. In most of our calculations we set $E^i = 0$, since the projectile energies are in comparison much larger. We will test this assumption. Since we are considering the optical potential in the impulse approximation, we neglect the mean field W_i of Eq. (2.2) in the following.

The driving term of Eq. (2.1) denotes the optical potential, which in first order is given as

$$\langle \mathbf{k}'|\langle\Phi_A|PUP|\Phi_A\rangle|\mathbf{k}\rangle \equiv \hat{U}(\mathbf{k}',\mathbf{k}) = \sum_{i=n,p} \langle \mathbf{k}'|\langle\Phi_A|\hat{\tau}_{0i}(\mathcal{E})|\Phi_A\rangle|\mathbf{k}\rangle. \tag{2.3}$$

Here $\mathbf{k}'$ and $\mathbf{k}$ are the external momenta of the system, $\hat{\tau}_{0i}(\mathcal{E})$ represents the NN transition operator

$$\hat{\tau}_{0i}(E) = v_{0i} + v_{0i} g_i(E) \hat{\tau}_{0i}, \tag{2.4}$$

with

$$g_i(E) = [(E - E^i) - h_0 - h_i + i\varepsilon]^{-1}, \tag{2.5}$$

and v_{0i} representing the NN interaction. The sum over i in Eq. (2.3) indicates the two different cases, namely when the target nucleon is one of Z protons, and when it is one of N neutrons. The energy $\mathcal{E}$ is the energy of the interacting system. Inserting a complete set of momenta for the struck target nucleon before and after the collision and evaluating the momentum conserving δ-functions gives as final expression for the full-folding optical potential [6,7]

$$\hat{U}(\mathbf{q},\mathbf{K}) = \sum_{i=n,p} \int d^3P\, \eta(\mathbf{P},\mathbf{q},\mathbf{K})\, \hat{\tau}_{0i}(\mathbf{q}, \frac{1}{2}(\frac{A+1}{A}\mathbf{K} - \mathbf{P}), \mathcal{E})$$

$$\rho_i(\mathbf{P} - \frac{A-1}{A}\frac{\mathbf{q}}{2}, \mathbf{P} + \frac{A-1}{A}\frac{\mathbf{q}}{2}). \tag{2.6}$$

Here the arguments of the NN amplitude $\hat{\tau}_{0i}$ are $\mathbf{q} = \mathbf{k}' - \mathbf{k} = \mathcal{K}' - \mathcal{K}$ and $\frac{1}{2}(\mathcal{K}' + \mathcal{K}) = \frac{1}{2}(\frac{A+1}{A}\mathbf{K} - \mathbf{P})$, where $\mathcal{K}' = \frac{1}{2}(\mathbf{k}' - (\mathbf{P} - \frac{\mathbf{q}}{2} - \frac{\mathbf{K}}{A})$ and $\mathcal{K} = \frac{1}{2}(\mathbf{k} - (\mathbf{P} + \frac{\mathbf{q}}{2} - \frac{\mathbf{K}}{A})$ are the nonrelativistic final and initial nuclear momentum in the zero momentum frame of the NN system, and $\mathbf{K} = \frac{1}{2}(\mathbf{k}' + \mathbf{k})$. The factor $\eta(\mathbf{P},\mathbf{q},\mathbf{K})$ is the Møller factor for the frame transformation [8],

and ρ_i represents the density matrix of the target. Evaluating the propagator $g_i(E)$ of Eq. (2.5) in the nucleon-nucleus (NA) center of mass frame yields for the energy argument $\mathcal{E}$ of the NN amplitude $\hat{\tau}_{0i}$ of Eq. (2.6)

$$\mathcal{E} = E_{NA} - \frac{(\frac{A-1}{A}\mathbf{K} + \mathbf{P})^2}{4m_N}. \tag{2.7}$$

Here E_{NA} is the total energy in the NA center of mass frame and m_N is the nucleon mass. At this point we assume $E^i = 0$ as was discussed earlier. Since we employ relativistic definitions for the NA kinematics we have $E_{NA} = \sqrt{(\mathbf{k}c)^2 + (m_N c^2)^2} + \sqrt{(-\mathbf{k}c)^2 + (m_A c^2)^2}$, where m_A denotes the mass of the nucleus. With these definitions, the optical potential of Eq. (2.6) becomes

$$\hat{U}(\mathbf{q}, \mathbf{K}) = \sum_{i=n,p} \int d^3 P \eta(\mathbf{P}, \mathbf{q}, \mathbf{K}) \, \hat{\tau}_{0i}(\mathbf{q}, \frac{1}{2}(\frac{A+1}{A}\mathbf{K} - \mathbf{P}), E_{NA} - \frac{(\frac{A-1}{A}\mathbf{K} + \mathbf{P})^2}{4m_N})$$
$$\rho_i(\mathbf{P} - \frac{A-1}{A}\frac{\mathbf{q}}{2}, \mathbf{P} + \frac{A-1}{A}\frac{\mathbf{q}}{2}). \tag{2.8}$$

This expression shows that the evaluation of the full-folding integral requires the NN t-matrix not only off-shell but also at energies $E_{NA} \geq \mathcal{E} > -\infty$. Specifically when going to negative energies, we have to take into account the pole structure of the NN t-matrix. The NN interaction supports a bound state at $E_d = -2.225$ MeV in the $^3S_1 - ^3D_1$ channel, the deuteron, and a virtual state in the $^1S_0$ channel at -66 keV, the 'di-proton'. A virtual state means a pole of the NN t-matrix in the second sheet of the complex energy plane, which manifests itself on the real axis as a very narrow finite peak (about 100 keV wide) around the pole position. The deuteron, a true bound state, causes a pole in the NN t-matrix at the binding energy E_d. In order to explicitly treat this pole, we factorize $\hat{\tau}_{0i}$ into a pole term and a residue function

$$\bar{\tau}_{0i} = \hat{\tau}_{0i} \times (E_{NA} - \frac{(\frac{A-1}{A}\mathbf{K} + \mathbf{P})^2}{4m_N} - E_d), \tag{2.9}$$

so that the optical potential takes the form

$$\hat{U}(\mathbf{q}, \mathbf{K}) = \sum_{i=n,p} \int d^3 P \frac{\bar{\tau}_{0i}(\mathbf{q}, \frac{1}{2}(\frac{A+1}{A}\mathbf{K} - \mathbf{P}), E_{NA} - \frac{(\frac{A-1}{A}\mathbf{K}+\mathbf{P})^2}{4m_N})}{E_{NA} - \frac{(\frac{A-1}{A}\mathbf{K}+\mathbf{P})^2}{4m_N} - E_d + i\epsilon}$$
$$\eta(\mathbf{P}, \mathbf{q}, \mathbf{K})\rho_i(\mathbf{P} - \frac{A-1}{A}\frac{\mathbf{q}}{2}, \mathbf{P} + \frac{A-1}{A}\frac{\mathbf{q}}{2}). \tag{2.10}$$

To obtain a simple pole, which can be treated with standard numerical methods, we perform a change of the integration variable to $\mathbf{Q} = \frac{A-1}{A}\mathbf{K} + \mathbf{P}$, and Eq. (2.10) becomes

$$\hat{U}(\mathbf{q}, \mathbf{K}) = \sum_{i=n,p} \int d\hat{Q} \int_0^\infty dQ Q^2 \, 4m_N \frac{\bar{\tau}_{0i}(\mathbf{q}, \frac{1}{2}(2\mathbf{K} - \mathbf{Q}), E_{NA} - \frac{Q^2}{4m_N})}{Q_d^2 - Q^2 + i\epsilon}$$
$$\eta(\mathbf{Q}, \mathbf{q}, \mathbf{K})\rho_i(\mathbf{Q} - \frac{A-1}{A}(\mathbf{K} + \frac{\mathbf{q}}{2}), \mathbf{Q} - \frac{A-1}{A}(\mathbf{K} - \frac{\mathbf{q}}{2}))$$

4

$$= \sum_{i=n,p} \int d\hat{Q} \, \mathcal{P} \int_0^\infty dQ Q^2 \, 4m_N \frac{\bar{\tau}_{0i}(\mathbf{q}, \frac{1}{2}(2\mathbf{K} - \mathbf{Q}), E_{NA} - \frac{Q^2}{4m_N})}{Q_d^2 - Q^2}$$

$$\eta(\mathbf{Q}, \mathbf{q}, \mathbf{K})\rho_i(\mathbf{Q} - \frac{A-1}{A}(\mathbf{K} + \frac{\mathbf{q}}{2}), \mathbf{Q} - \frac{A-1}{A}(\mathbf{K} - \frac{\mathbf{q}}{2}))$$

$$-i \sum_{i=n,p} \int d\hat{Q} \, 2\pi m_N Q_d \, \bar{\tau}_{0i}(\mathbf{q}, \frac{1}{2}(2\mathbf{K} - Q_d\hat{Q}), E_d)$$

$$\eta(Q_d\hat{Q}, \mathbf{q}, \mathbf{K})\rho_i(Q_d\hat{Q} - \frac{A-1}{A}(\mathbf{K} + \frac{\mathbf{q}}{2}), Q_d\hat{Q} - \frac{A-1}{A}(\mathbf{K} - \frac{\mathbf{q}}{2})). \quad (2.11)$$

Here $\int d\hat{Q}$ represents the angular integration, $Q_d = \sqrt{4m_N(E_{NA} - E_d)}$, and $\mathcal{P}$ denotes a Cauchy principal value integral.

The cut in the integrand of Eq. (2.11) indicates the opening of a new channel in the scattering reaction. In this specific case it is the deuteron pickup channel, describing when an incoming projectile proton picks up a neutron and a deuteron is knocked out, thus removing flux from the elastic channel. In order to obtain some a priori estimate on the possible size of this additional channel on the elastic scattering reaction, it is worthwhile to look at experimental information on the deuteron pickup reaction.

In the 1980's cross sections of the (p,d) reaction have been measured for the closed shell nuclei considered here [9–11]. For ^{40}Ca at 200 MeV, the differential cross section for the (p,d) reaction for small angles (10-20 degrees) is about 1 mb/sr while at 65 MeV it is about 10 mb/sr. Compared to the typical size of differential cross sections for elastic scattering in a similar angular range (cp. Figs. 2 and 6), this is quite small. The effect of this additional channel will be studied in our calculations of elastic scattering observables and compared to calculations where the integration variable is decoupled from the energy of propagation of the projectile and target target nucleon. The latter is an approximation where the energy of the NN t-matrix is fixed at half the beam energy in the laboratory frame

$$\mathcal{E} = E_0 = \frac{1}{2}\frac{k_{lab}^2}{2m_N} = \frac{1}{2}\frac{(\frac{A+1}{A}k_0)^2}{2m_N}, \quad (2.12)$$

where k_{lab} and k_0 are the on-shell momenta in the laboratory and NA system respectively. With this fixed energy approximation the full-folding optical potential of Eq. (2.10) becomes

$$\hat{U}(\mathbf{q}, \mathbf{K}) = \sum_{i=n,p} \int d^3P \eta(\mathbf{P}, \mathbf{q}, \mathbf{K}) \, \hat{\tau}_{0i}(\mathbf{q}, \frac{1}{2}(\frac{A+1}{A}\mathbf{K} - \mathbf{P}), E_0)$$

$$\rho_i(\mathbf{P} - \frac{A-1}{A}\frac{\mathbf{q}}{2}, \mathbf{P} + \frac{A-1}{A}\frac{\mathbf{q}}{2}). \quad (2.13)$$

Full-folding calculations based on this approximation have been carried out by several groups [6,12].

Fixing the energy at E_0 as given in Eq. (2.12) is a 'historic' choice, made by all calculations based on the KMT formulation [13]. The argument for this specific choice of E_0 is, that this is the energy at which free NN scattering at a fixed target nucleon would occur. This choice of E_0 favors the forward scattering process, and it was argued that due to the narrow peaking of the density in momentum space, the scattering is dominated by forward scattering. Having in mind that the differential cross section for e.g. proton scattering

from ^{208}Pb at 200 MeV falls off by five orders of magnitude between 5 and 30 degrees, this argument may capture some truth, however needs to be tested numerically.

Before discussing the results of our calculations, we would like to elaborate some more on the details of our numerical implementation. Treating the pole structure of the NN t matrix while integrating over the energy of the propagation is standard in modern three-nucleon scattering calculations [14]. However, these calculations are carried out in partial waves, which allows treating the $^3S_1 - {}^3D_1$ and $^1S_0$ channel separately. Our calculation of the full-folding optical potential of Eq. (2.11) is carried out directly in three dimensions based on Monte Carlo integration. Thus, for the neutron-proton part of the optical potential, we have to treat the pole singularity and the virtual state simultaneously. The principle value integral of Eq. (2.11) is treated with standard subtraction techniques. When calculating the optical potential as given in Eq. (2.11), we have to interpolate the NN t-matrix in four dimensions, $|\mathbf{q}|, |2\mathbf{K} - \mathbf{Q}|, (2\mathbf{K} - \mathbf{Q}) \cdot \mathbf{q}$, and the energy. For the momenta we use a three dimensional B-spline, for the energy a linear interpolation, since over a large range of energies the NN t-matrix is a slowly varying function of the energy. When carrying out the energy integration of Eq. (2.11), we find that for the higher projectile energies integrating out to -100 MeV c.m. energy in the NN t-matrix is sufficient, while for the lower energies (65 MeV) we need to integrate out to -400 MeV c.m. energy.

Of course, the argument of the NN t-matrix being a slowly varying function of the energy is not true in the immediate vicinity of the virtual state in the $^1S_0$ channel. Since the peak around the pole position in the second energy sheet is finite and very narrow, we evaluate the integral over the t-matrix in this region separately and define

$$\hat{\tau}_{av,i}(\mathbf{q}, \mathbf{K}, E_{NA}) = \frac{1}{\Delta_1 + \Delta_2} \int_{Q_0 - \Delta_1}^{Q_0 + \Delta_2} dQ \hat{\tau}_{0i}(\mathbf{q}, \frac{2\mathbf{K} - \mathbf{Q}}{2}, E_{NA} - \frac{Q^2}{4m_N}), \qquad (2.14)$$

where Q_0 is defined via $E_{NA} - \frac{Q_0^2}{4m_N} = 0$, which is close to the pole position on the second sheet of the complex energy plane. The 'average' $\hat{\tau}_{av,i}$ is usually obtained from 40 energy points over a momentum interval of 0.5 MeV, and is then used as one of the interpolation points in the energy interpolation. The midpoint Q_0 for the integration in Eq. (2.14) depends via E_{NA} on the projectile energy, which implies that the averaging process has to be carried out for each projectile energy. If we want to simplify the numerical procedure and create $\hat{\tau}_{av,i}$ only once, we change the integration variable from Q to E and calculate

$$\hat{\tau}_{av,i}(\mathbf{q}, \mathbf{K}, E_0) = \frac{1}{2\delta_1} \int_{E_0 - \delta_1}^{E_0 + \delta_1} dE \hat{\tau}_{0i}(\mathbf{q}, \frac{2\mathbf{K} - \mathbf{Q}}{2}, E), \qquad (2.15)$$

where we have chosen $E_0 = 0$ MeV and $\delta_1 = 0.25$ MeV. The error in obtaining $\hat{\tau}_{av,i}$ from Eq. (2.15) instead of Eq. Eq. (2.14) is small if $\frac{2\delta_1}{E_{NA}}$ is small. For our worst case tested, $E_{NA} = 50$ MeV for proton scattering from ^{208}Pb the numerical error was 1%.

III. RESULTS AND DISCUSSION

In this paper the study of elastic scattering of protons from spin-zero target nuclei at energies that range from 65 to 200 MeV incident projectile energy is strictly first order in the spectator expansion and based on the impulse approximation. The full-folding optical

potential is calculated as outlined in the previous section, specifically as given in Eq. (2.11). As a model for the density matrix for the target nucleus we employ a Dirac-Hartree calculation [15]. The Fourier transform of the vector density, $\rho(\mathbf{r'}, \mathbf{r})$, serves as our non-relativistic single particle density [6]. Another crucial ingredient in the calculation of the optical potential, $\hat{U}(\mathbf{q}, \mathbf{K})$, is the fully off-shell NN t-matrix. The calculations presented here employ the NN t-matrix based on the charge-dependent Bonn potential [16]. This potential is fitted to describe the Nijmegen database with a χ^2 per datum ~ 1. It is also to be understood that we perform all spin summations in obtaining $\hat{U}(\mathbf{q}, \mathbf{K})$. This reduces the required NN t-matrix elements to a spin independent component (corresponding to the Wolfenstein amplitude A) and a spin-orbit component (corresponding to the Wolfenstein amplitude C). Since we are assuming that we have spin saturated nuclei, the components of the NN t-matrix depending on the spin of the struck nucleon vanish. The Coulomb interaction between the projectile and the target is included using the exact formulation as described in Ref. [17].

At first we want to concentrate on proton scattering from different target nuclei at an intermediate energy. In Fig. 1 we display the differential cross section $\frac{d\sigma}{d\Omega}$, the analyzing power A_y, and the spin rotation function Q, for elastic proton scattering from ^{16}O. The solid line represents the full calculation of the optical potential according to Eq. (2.11) and the dashed line shows the calculation where the energy of the NN t-matrix is fixed at half the projectile energy. It is remarkable how close the fixed energy result is to the full calculation. This may stem from a relatively weak energy dependence of the NN t-matrix and the fact that the folding with the sharply peaked density matrix does not sample the NN t-matrix in the negative energy region. We confirmed this numerically by artificially limiting the energy integration to positive energies and did not find noticeable effects in the scattering observables at 200 MeV. In Fig. 2 we show the observables for elastic proton scattering from ^{40}Ca at 200 MeV and in Fig. 3 those for elastic proton scattering from ^{208}Pb. As in Fig. 1, the solid line represents the full calculation of the optical potential taking the energy dependence of the NN t-matrix into account, whereas the dashed line shows the calculation at fixed energy E_0 given in Eq. (2.13). For all three nuclei the fixed energy result is remarkably close to the full calculation, a conclusion which essentially was also drawn in Ref. [4]. A general trend is that for the fixed energy calculation the dip structure in the differential cross section and the spin observables is slightly more pronounced.

In order to assess the importance of the additional energy shift given by E^i in Eq. (2.2), we show in Fig. 1 a calculation (including the energy dependence of the NN t-matrix), which was performed setting $E^i = -8$ MeV. This results in a shift of the total energy of the NA system to a slightly higher value, as suggested already in Refs. [18,19]. The effect of this energy shift is negligible at 200 MeV as shown in Fig. 1.

Next we turn to lower projectile energies, where we may expect to see differences between the full calculation including the energy dependence of the NN t-matrix and a calculation with a NN t-matrix energy fixed at half the projectile energy. In Fig. 4 we display the results for proton scattering from ^{208}Pb at 160 MeV and in Fig. 5 those for proton scattering from ^{16}O at 135 MeV. Compared to the results at 200 MeV, the difference between the solid line, which represents the full calculation, and the dashed line, which represents the calculation for a fixed energy of the NN t-matrix, becomes more pronounced, especially for A_y at larger angles as shown in Fig. 4. A similar figure is shown in Ref. [4], however a direct comparison between calculations is not possible, since different NN t-matrices as well

as densities are employed. The scattering observables given in Fig. 5 for proton scattering from ^{16}O at 135 MeV exhibit less difference between the solid and dashed lines, leading to the conclusion that even at this relatively low energy the fixed energy prescription in the optical potential is still amazingly and perhaps unexpectedly good. One common trend is becoming apparent in Figs. 4 and 5, namely that the differential cross sections predicted by the full calculations are systematically higher compared to the ones predicted by the calculations employing a NN t-matrix at a fixed energy. In Fig. 5 we also include a full calculation, in which the energy shift E^i is chosen to be $E^i = -8$ MeV (dash-dotted line). Again, we conclude that the effect of this energy shift is minute.

Last we want to consider scattering observables at an energy below 100 MeV projectile energy. It has already been stated in the literature [3,5,20] that at these low energies the strict impulse approximation is insufficient to describe the experimental observables. We arrive again at the same conclusion, when showing in Fig. 6 the scattering observables for proton scattering from ^{40}Ca at 65 MeV. However, this is not the main point we want to make. When comparing a calculation including the energy dependence of the NN t-matrix in the optical potential (solid line) with a calculation where the energy is fixed at half the projectile energy (dashed line), we clearly see that the additional channels, the deuteron pick-up channel and the di-proton state have a sizable effect on the elastic observables. This is consistent with the experimental data, which show that the cross section for the (p,d) reaction is getting larger at lower energies. The differential cross section predicted by the full calculation (solid line) is higher than the one predicted by the calculation using the fixed energy prescription (dashed line), and actually slightly closer to the experiment. The spin observables obtained from the full calculations show much less structure compared to those from the fixed energy calculation. However, both impulse approximation calculations do not adequately describe the spin observables. A similar conclusion was drawn in Ref. [5], although there the effect of including the deuteron and di-proton channel is more dramatic than in our calculations. For the first time we also observe a visible effect on the scattering observables, when we introduce an energy shift by setting $E^i = -8$ MeV (dash-dotted line).

From Fig. 6 we see that he impulse approximation, even if accurately and completely calculated, is clearly inadequate in describing the elastic scattering observables at such a low energy, and additional effects have to be included. The first term in the spectator expansion contains as additional term the coupling of the struck target nucleon to the residual nucleus [3]. For comparison we include a calculation in Fig. 6 as dotted line, where this term is calculated in an approximate fashion as described in Ref. [19]. We see that this additional 'medium' contribution is necessary to get a better description of the spin observables.

IV. CONCLUSION

We have calculated the full-folding integral for the first-order optical potential using the impulse approximation within the framework of the spectator expansion of multiple scattering theory. The exact calculation of this full-folding integral requires a three-dimensional integration, in which the integration variable is coupled to the energy of propagation of the projectile and target nucleon. We have carried out the calculation taking into account the pole structure of the NN t-matrix when integrating to negative energies. Our optical

potentials are based on a Dirac-Hartree model for the nuclear density matrix and the charge-dependent Bonn potential for the NN t-matrix. Recoil and frame transformation factors are implemented in the calculation in their complete form. We calculate elastic scattering observables for ^{16}O, ^{40}Ca, and ^{208}Pb at projectile energies from 65 to 200 MeV laboratory energy and compare the full calculation with calculations in which the energy of the NN t-matrix is fixed at half the projectile energy. We find that this fixed energy prescription describes the full calculation remarkably well for proton scattering at 200 MeV projectile energy. This leads to the conclusion that the pole structure of the NN t-matrix does not play a role at intermediate energies. For projectile energies below 200 MeV we find that the influence of the deuteron and di-proton state slowly gains importance as we approach lower energies. However, between 100 and 200 MeV these effects are still relatively small. This is consistent with the small size of the experimentally measured cross sections for the (p,d) reaction. At 65 MeV we see considerable differences between the full calculation and the one in which the energy is kept fixed. In general, we find smaller differences between our full calculation and the fixed energy calculations as were suggested in Ref. [4].

The calculations presented in this manuscript are strictly based on the impulse approximation using the free NN t-matrix. It has been stated in many places that the impulse approximation is insufficient at energies around 100 MeV projectile energy. We confirm this result, while carrying out complete calculations of the optical potential taking into account the energy dependence of the NN t-matrix. Additional corrections have to be taken into account at lower energies. Within the framework of the spectator expansion these corrections have been derived and carried out in an approximate fashion [3]. A similarly complete calculation, as given here for the first order term in the impulse approximation, will require a complete Faddeev calculation of the correction term, which is at present not possible.

REFERENCES

[1] D.J. Ernst, J.T. Londergan, G.A. Miller, and R.M. Thaler, Phys. Rev. **C16**, 537 (1977).

[2] E.R. Siciliano and R.M. Thaler, Phys. Rev. **C16**, 1322 (1977).

[3] C.R. Chinn, Ch. Elster, R.M. Thaler, and S.P. Weppner, Phys. Rev. **C52**, 1992 (1995).

[4] H.F. Arellano, F.A. Brieva, and W.G. Love, Phys. Rev. **C50**, 2480 (1994).

[5] H.F. Arellano, F.A. Brieva, and W.G. Love, Phys. Rev. **C52**, 301 (1995).

[6] Ch. Elster, S.P. Weppner, and C.R. Chinn, to appear in Phys. Rev. C, and *http://xxx.lanl.gov/ps/nucl-th/9611045*.

[7] S.P. Weppner, Ph.D. Thesis, Ohio University, August 1997.

[8] C.J. Joachain, 'Quantum Collision Theory' (North-Holland Physics 1987) p. 387.

[9] K. Hosono *et al.*, Nucl. Phys. **A343**, 234 (1980).

[10] R. Abegg *et al.*, Phys. Rev. **C39**, 65 (1989).

[11] J.J. Kraushaar, J.R. Shepard, D.W. Miller, W.W. Jacobs, W.P. Jones, and D.W. Devins, Nucl. Phys. **A394**, 118 (1983).

[12] R. Crespo, R.C. Johnson, and J.A. Tostevin, Phys. Rev. **C41**, 2257 (1990).

[13] A. Kerman, M. McManus, and R. M. Thaler, Ann. Phys. **8**, 551 (1959).

[14] H. Witala, T. Cornelius, and W. Glöckle, Few-Body Systems **3**, 123 (1988).

[15] C.J. Horowitz and B.D. Serot, Nucl. Phys **A368**, 503 (1981).

[16] R. Machleidt, F. Sammarruca, Y. Song, Phys. Rev. **C53**, R1483 (1996).

[17] C.R. Chinn, Ch. Elster, and R.M. Thaler, Phys. Rev. **C44**, 1569 (1991).

[18] R. Crespo, R.C. Johnson, and J.A. Tostevin, Phys. Rev. **C48**, 351 (1993).

[19] C.R. Chinn, Ch. Elster, R.M Thaler, Phys. Rev. **C48**, 2956 (1993).

[20] H.F. Arellano, F.A. Brieva, M. Sander, H.V. von Geramb, Phys. Rev. **C54**, 2570 (1996).

[21] E.J. Stephenson, in 'Antinucleon- & Nucleon-Nucleus Interactions' Telluride, Co. 1985, pp 299, ed. by G. Walker et al. (Plenum Press, NY, 1985).

[22] H.O. Mayer, P. Schwandt, G.L. Mooke, P.P. Singh, Phys. Rev. **C23**, 616 (1981); H.O. Mayer, P. Schwandt, W.W. Jacobs, J.R. Hall, Phys. Rev. **C27**, 459 (1983).

[23] D.A. Hutcheon et al. in 'Polarization Phenomena in Nuclear Physics - 1980', Proceedings of the Fifth International Symposium on Polarization Phenomena in Nuclear Physics, AIP Conf. Proc. No. 69, edited by G.G. Ohlson, R.E. Brown, N. Jarmie, W.W. McNaughton, and G.M. Hale (AIP, NY, 1981), p. 454. The data for Q are from Na Gi, Masters Thesis, Simon Frazer University, British Columbia, 1987.

[24] A. Nadasen, P. Schwandt, P.P. Singh, W.W. Jacobs, A.D. Bocher, P.T. Debevec, M.D. Katchuck, J.T. Meek, Phys. Rev. **C23**, 1023 (1981); P. Schwandt, H.O. Mayer, W.W. Jacobs, A.D. Baches, S.E. Vigdor, M.D. Kartchuck, Phys. Rev. **C26**, 55 (1982).

[25] J. Kelly et al. Phys. Rev. Let. **45**, 2012 (1980) ; K. Amos et al., Nucl. Phys. **A413**, 255 (1984).

[26] H. Sakaguchi, M. Nakamura, K. Hatanaka, A. Goto, T. Noro, F. Ohtani, H. Sakamoto, H. Ogawa, and S. Kobayashi, Phys. Rev. **C 26**, 944 (1982).

FIGURES

FIG. 1.   The angular distribution of the differential cross-section ($\frac{d\sigma}{d\Omega}$), analyzing power (A_y) and spin rotation function (Q) are shown for elastic proton scattering from ^{16}O at 200 MeV laboratory energy. The solid line represents the calculation performed with a first-order full-folding optical potential based on the DH density [15] and the CD-Bonn model [16] including the energy dependence of the NN t-matrix. The dashed line represents a calculation where the energy of the NN t-matrix is fixed at half the projectile energy. The dash-dotted line stands for a calculation including the energy dependence of the NN t-matrix and an additional energy shift by $E^i = -8$ MeV. The data are taken from Ref. [21].

FIG. 2. Same as Fig. 1, except that the target nucleus is ^{40}Ca, and the dash-dotted line is omitted. The data are taken from Ref. [22].

FIG. 3. Same as Fig. 2, except that the target nucleus is ^{208}Pb. The data are taken from Ref. [22].

FIG. 4. Same as Fig. 3, except for ^{208}Pb at 160 MeV proton kinetic energy. The data are taken from Ref. [24].

FIG. 5. Same as Fig. 1, except for ^{16}O at 135 MeV proton kinetic energy. The data are taken from Ref. [25].

FIG. 6. Same as Fig. 1, except for ^{40}Ca at 65 MeV proton kinetic energy. The additional dotted line denotes a calculation including the effect of the coupling of the struck target nucleon to the residual nucleus. The data are taken from Ref. [26].
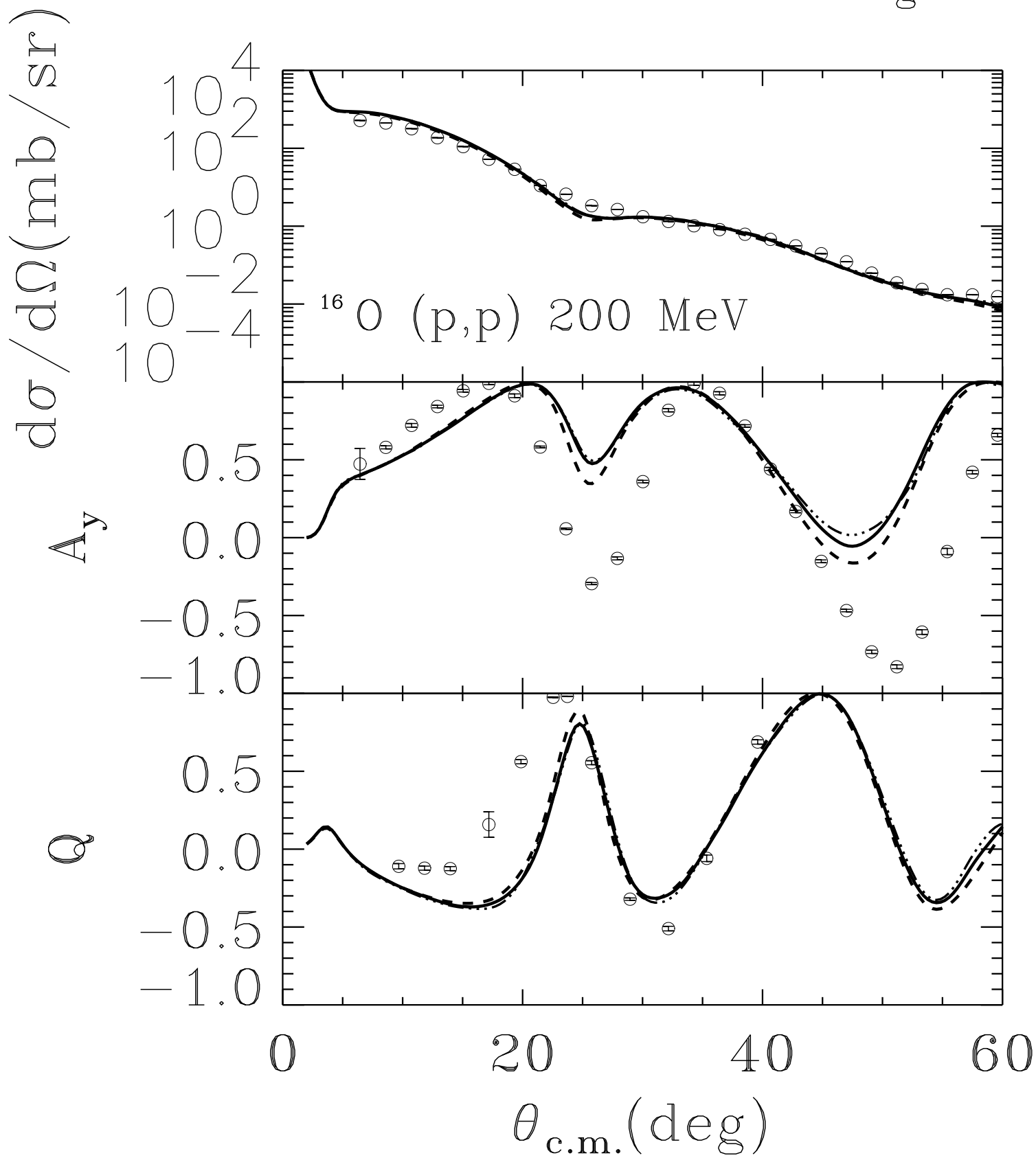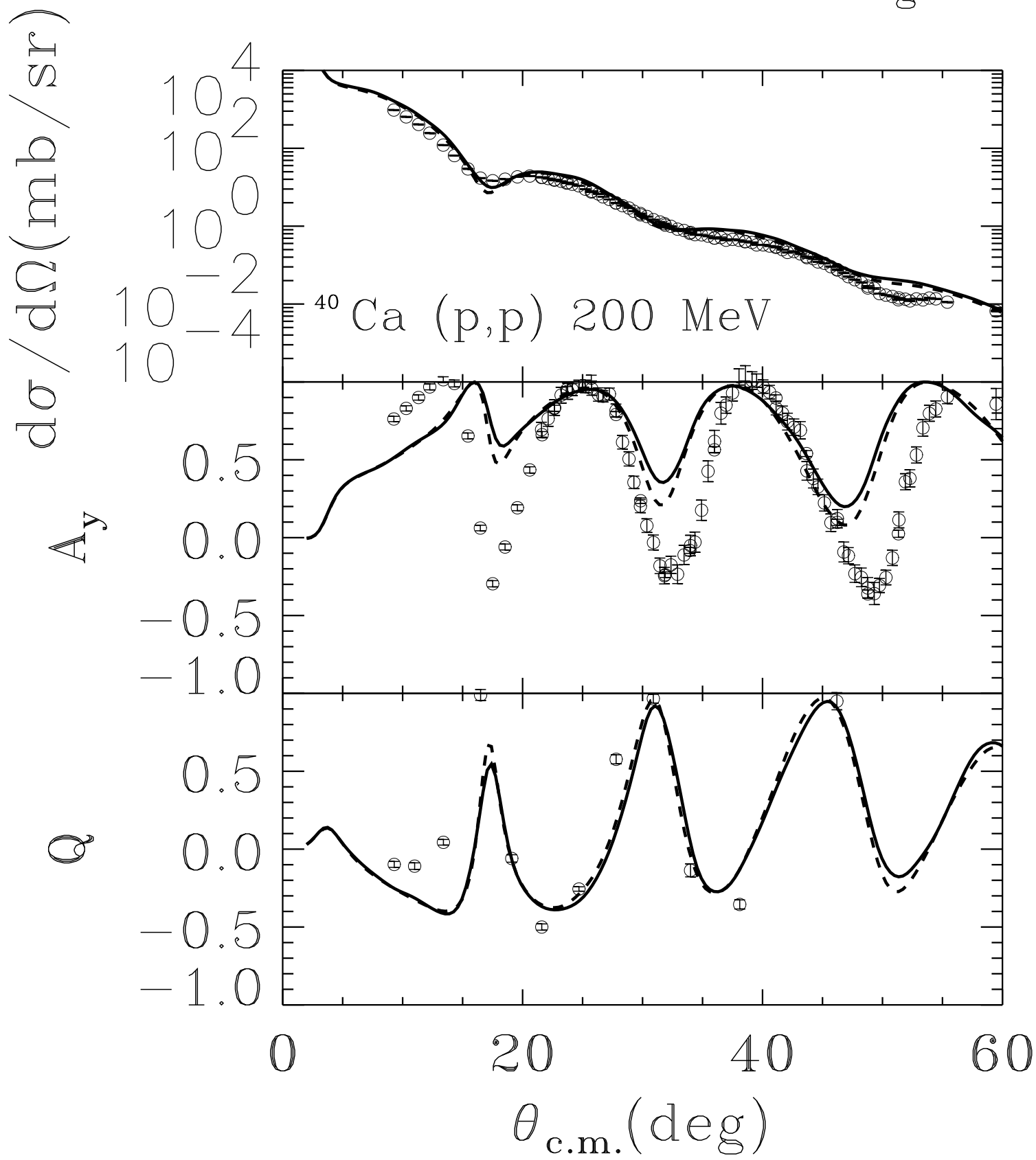
Fig. 1

^{16}O (p,p) 200 MeV
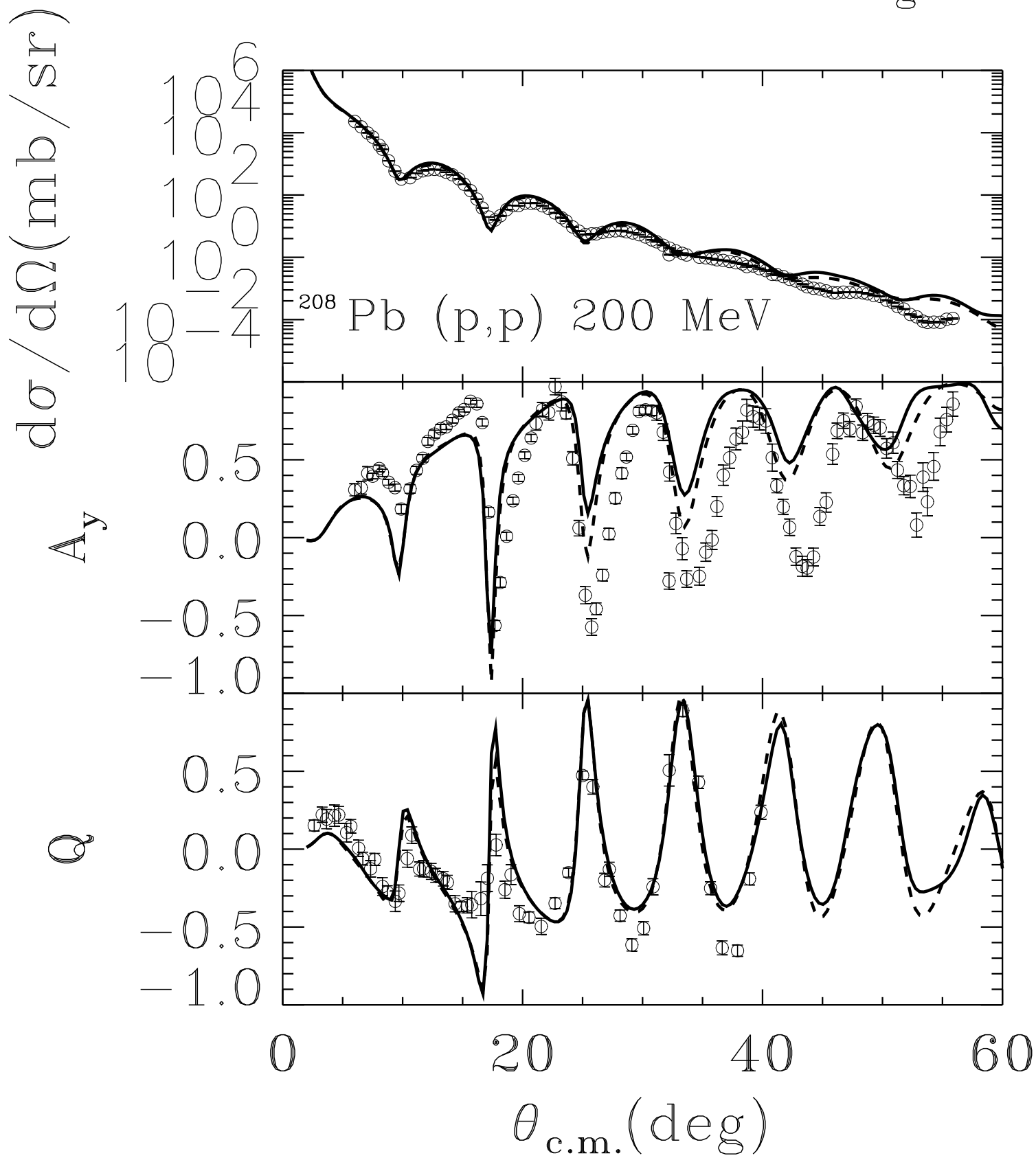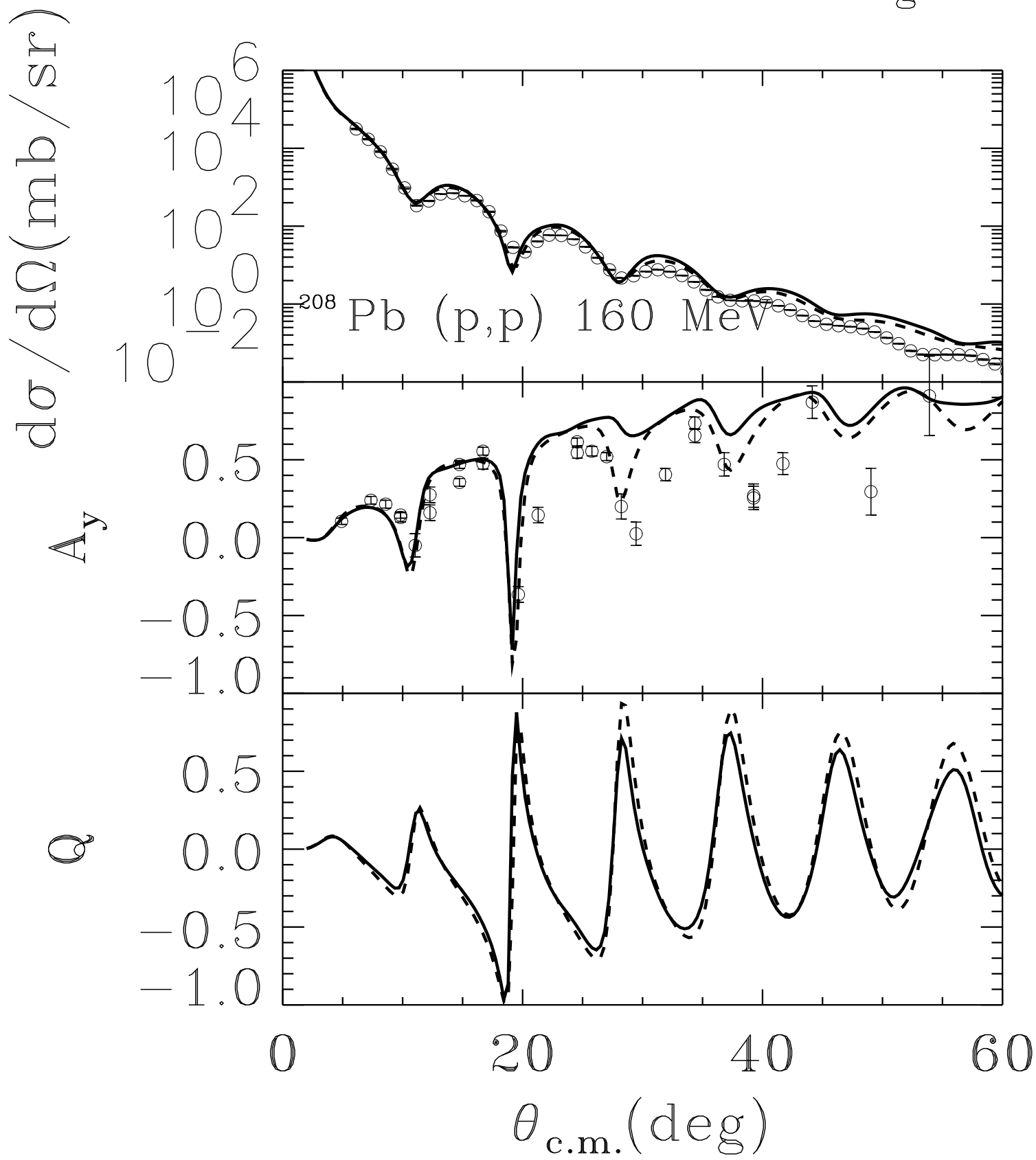
Fig. 2

^{40}Ca (p,p) 200 MeV

Fig. 3

^{208}Pb (p,p) 200 MeV

Fig. 4

^{208}Pb (p,p) 160 MeV

Fig. 5

^{16}O (p,p) 135 MeV

Fig. 6

^{40}Ca (p,p) 65 MeV